

A new, evolved bipolar planetary nebula^{*}

Romano L.M. Corradi¹, Eva Villaver¹, Antonio Mampaso¹, and Mario Perinotto²

¹ Instituto de Astrofísica de Canarias, c. Via Lactea S/N, E-38200 La Laguna, Tenerife, Spain

² Dipartimento di Astronomia e Scienza dello Spazio, Università di Firenze, Largo E. Fermi 5, I-50125 Firenze, Italy

Received 9 December 1996 / Accepted 3 February 1997

Abstract. Optical imaging and spectroscopy reveal that the ionised region No.252 in the list of Marsalkowa (1974), whose photograph is presented in the “Atlas of Galactic Nebulae” by Neckel & Vehrenberg (1990), is actually a planetary nebula. According to Acker et al. (1992), the object should therefore be named as PN G321.6+02.2. The nebula has the following properties: it is located at 2.0 ± 0.5 kpc from the Sun, has a bipolar morphology, a giant size (~ 4 pc!), low densities, a hot (unobserved) central star ($T > 130000$ K), and extreme He and N overabundances ($\text{He}/\text{H} = 0.147 \pm 0.029$, $\log(\text{N}/\text{O}) = 0.47^{+0.20}_{-0.38}$). The nebula is likely to be in a very evolved evolutionary stage.

Key words: planetary nebulae: PN G321.6+02.2

1. Introduction

In recent years, several papers have been devoted to the study of bipolar planetary nebulae (PNe). While their morphological and dynamical properties are successfully modelled by the current hydrodynamical theories for PN formation and evolution (Balick & Frank 1997), the original mechanism driving the asymmetrical outflow from the AGB progenitor has not been established yet. In this respect, collimating processes caused by a variety of binary interactions are still the favourite model to produce this kind of nebulae (Livio 1997). According to several observational properties, it has also been recognized that bipolar nebulae are associated with the highest mass progenitors of PNe (see Corradi & Schwarz 1995, hereafter CS95, for a discussion and list of references). Up to date, about 60 bipolar PNe are known (43 from the list of CS95, plus another ~ 15 new ones in Machado et al. 1996).

Included in the “Atlas of Galactic nebulae” by Neckel & Vehrenberg (1990), a photograph of the object No.252 in the list of Marsalkowa (1974) attracted our attention because of its strong similarity with two bipolar PNe, K 1–10 and NGC 2899 (see Fig. 2 in CS95). No references on the object are quoted in

the SIMBAD database. In addition, the nebula is not known as an IRAS source, nor CO and radio data exist in the literature which are detailed enough to verify possible associations with HII regions or molecular clouds. We have therefore decided to obtain optical CCD images and spectra of the object, and the subsequent analysis confirmed that the object is indeed a planetary nebula. These observations are discussed in detail in the following sections.

2. Observations

Images and spectra of the nebula were obtained at the 3.5m NTT ESO telescope with the EMMI multimode instrument during April 1996. The detector was the TEK 2048² CCD ESO#36, which provides a spatial scale of $0''.27 \text{ pix}^{-1}$. Two 5 min [NII] images of the nebula were obtained and averaged together. The central wavelength and FWHM of the [NII] filter are of 658.8 and 3.0 nm. The seeing during observations was excellent: $0''.7$ FWHM.

A high resolution long-slit spectrum was obtained using the EMMI-REMD with the echelle grating #14, which gives a reciprocal dispersion of $0.004 \text{ nm pix}^{-1}$, or a resolving power of 60000 with the adopted slit width of $1''.0$. The spectral order including $\text{H}\alpha$ and both the [NII] forbidden lines was isolated by means of a narrowband filter centred at 656.8 nm and with a FWHM of 7.3 nm (see Corradi et al. 1996 for more information about long slit echelle spectroscopy with NTT+EMMI). The long slit of EMMI (6 arcmin) was located at position angle $+36^\circ$, passing through the NW side of the equatorial waist of the bipolar nebula (Fig. 1). The exposure time was 30 min.

Two 10 min low-resolution spectra were then obtained, and averaged together, with the slit passing through the brightest part of the nebula (SE side of the equatorial waist; see Fig. 1) at P.A. $+14^\circ$. Grism #3 was used, covering a spectral range from 390.0 nm to 870.0 nm with a reciprocal dispersion of 0.22 nm pix^{-1} , and a resolving power of 750 (slit width $1''.0$). A spectrophotometric standard star was also observed.

Images and spectra were reduced using the standard procedures in the MIDAS package. In the low resolution spectrum, in order to increase the S/N ratio for the faintest lines, one-dimensional spectrum corresponding to $13''$ in the bright equa-

Send offprint requests to: R. Corradi (rcorradi@iac.es)

* Based on observations made at the European Southern Observatory

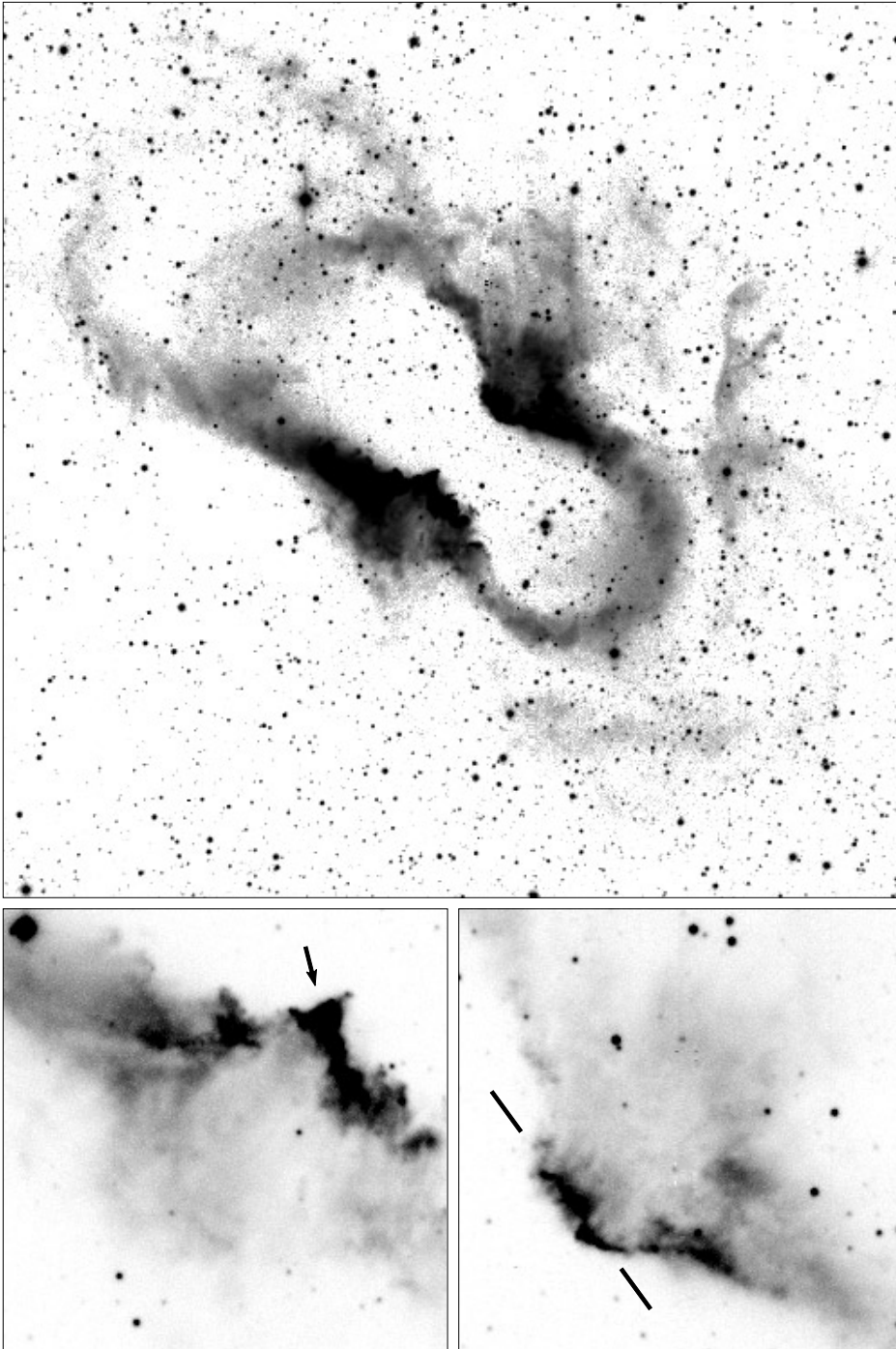


Fig. 1. At the top, the [NII] image of the whole nebula. At the bottom, enlargements of the two bright sides of its equatorial waist. In the left image, an arrow indicates the region of the nebula from which the 1-D low-resolution spectrum has been extracted (see text). In the right one, the solid lines indicate the location of the inner part of the 6' slit as it was positioned in the high-resolution spectrum. The main image (400'' \times 400'') is on a logarithmic intensity scale, the smaller ones (67'' \times 67'') on a linear scale. North is at the top, East to the left.

torial region was extracted by spatial binning. Line fluxes F_λ were then measured using the MIDAS/ALICE package. They are given in Table 1. From the comparison of the measurements in the two original spectra, errors on line fluxes have been estimated to range from about 10% for the brightest lines ($F_\lambda \geq 5 \cdot F_{H\beta}$) to 30% for the faintest ones ($F_\lambda \leq 0.5 \cdot F_{H\beta}$).

3. Results

3.1. Morphology

The [NII] image of the nebula is presented in Fig. 1. The object has a typical bipolar morphology, being composed of two faint lobes departing from a brighter equatorial waist. The northern lobe is partially broken, and faint filaments surround the main “hourglass” nebula. These outer structures might be evidence of either previous mass loss events or a blow-out of the main

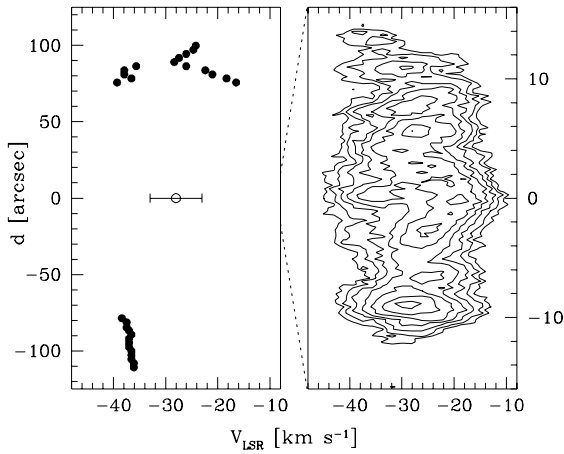


Fig. 2. To the left, the position-velocity plot for the outer parts of the nebula. Dots indicate radial velocities as computed by Gaussian fitting of the [NII]658.3 line in various positions throughout the limb of the lobes intersected by the slit. North is at the top. The empty circle indicates the systemic velocity of the nebula and its error. To the right, an enlargement of the inner 30'' of the slit, corresponding to the NW inner edge of the equatorial waist; the velocity profiles are displayed in form of iso-intensity contours of the [NII] line, with successive levels incrementing of a factor $\sqrt{2}$.

Table 1. Observed line fluxes, normalized to $F_{H\beta}=100$. The absolute $H\beta$ flux is $3.07 \times 10^{-15} \text{ erg cm}^{-2} \text{ s}^{-1}$.

| Ident. | F_λ | Ident. | F_λ |
|--------|---------------|--------|----------------|
| 434.05 | H γ 25 | 636.38 | [OI] 14 |
| 468.57 | HeII 45 | 654.80 | [NII] 2061 |
| 486.13 | H β 100 | 656.28 | H α 684 |
| 495.89 | [OIII] 256 | 658.34 | [NII] 6376 |
| 500.68 | [OIII] 792 | 667.90 | HeI+HeII 14 |
| 520.00 | [NI] 20 | 671.65 | [SII] 313 |
| 575.46 | [NII] 63 | 673.08 | [SII] 264 |
| 587.57 | HeI 26 | 713.58 | [ArIII] 122 |
| 630.03 | [OI] 66 | 732.50 | [OII] blend 23 |
| 631.21 | [SIII] 14 | | |

bipolar nebula, but the present data cannot distinguish between the two possibilities.

As typical of many bipolar PNe (CS95), a point-symmetrical distribution of light emission is observed in the equatorial regions of the object, with brightness enhancements along the SW and NE edges of the hourglass nebula. The equatorial waist has sharp, bright inner edges, while it extends outward for about 1' on each side forming a point-symmetrical equatorial "bulge". The long axis of the hourglass nebula has an apparent size of 4'.2; including the outer faint structures, the total extent of the nebula is more than 7'.

3.2. Kinematics

Radial velocities along the slit have been computed from the [NII]658.3 line. Note that the location of the slit was almost parallel to the long axis of the nebula, with an offset of 22'' from

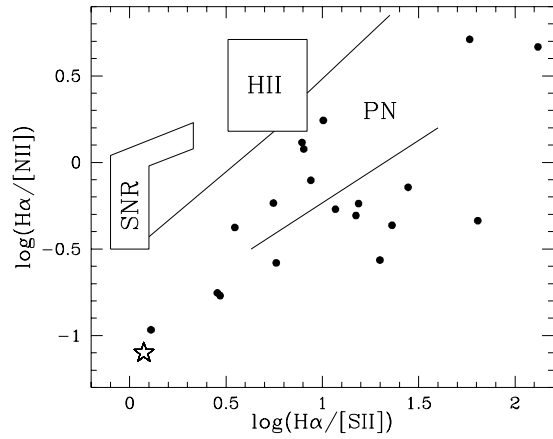


Fig. 3. The diagnostic diagram by Cantó (1981), for the observed nebula (star) and for 19 bipolar PNe (dots).

its symmetry and passing through the NW side of the equatorial waist. The position-velocity plot is presented in Fig. 2. The overall velocity range is of 25 km s^{-1} . The kinematical information is fragmentary, so that a detailed spatio-kinematical analysis of the kind of that presented in Corradi & Schwarz (1993), using the model from Solf & Ulrich (1985), cannot be applied. Some indications can however be derived from the comparison with that model. The small velocity difference between the two lobes indicate a small inclination angle of the nebula on the plane of the sky, and the modest velocity splitting observed in the northern lobe shows that the polar expansion velocities cannot be very high. Velocities of a few hundreds km s^{-1} , as observed in several bipolar PNe (CS95), can therefore be excluded, and a conservative upper limit of 100 km s^{-1} is adopted. Inside the equatorial waist, the velocity pattern is irregular and line profiles are in some positions double-peaked, with a velocity range of 20 km s^{-1} . The systemic velocity of the nebula, adopted as the mean velocity in the equatorial waist and corrected to the Local Standard of Rest, is $V_{LSR} = -28 \pm 5 \text{ km s}^{-1}$. The object is located close to the Galactic plane at a favourable longitude ($l=321^\circ.6$) to obtain an estimate of its distance by assuming that it participates to the general circular rotation around the Galactic centre. Assuming a standard Galactic rotation curve (cf. CS95), the kinematical distance of the nebula is then computed to be of $2.0 \pm 0.5 \text{ kpc}$.

3.3. Diagnostic diagram

Line fluxes from the low resolution spectrum have been used to compute the physico-chemical properties of the nebula, and the usual diagnostic diagrams for emission regions have been applied to check its possible classification as a PN. A glance at the spectrum clearly supports this hypothesis: the HeII468.6 line is quite strong relatively to H β , suggesting the existence of a high temperature source as typical of PNe. Note also that the [NII]/H α ratio is very large (~ 12), and the [SII] lines are relatively strong.

Table 2. Computed properties. Coordinates are given for the centre of symmetry of the nebula.

| | |
|--------------------------------|---------------------------------|
| $\alpha_{2000}, \delta_{2000}$ | 15 09 24 -55 33 03 |
| l, b | 321.6 2.2 |
| V_{LSR} | $-28 \pm 5 \text{ km s}^{-1}$ |
| Distance | $2.0 \pm 0.5 \text{ kpc}$ |
| Size | 4.1 pc |
| c_β | 1.23 |
| N_e | 250 cm^{-3} |
| T_e | $9600_{-600}^{+1000} \text{ K}$ |
| T_{EB} | $>130000 \text{ K}$ |

We have compared the position of the object with that of 19 bipolar PNe (Corradi et al., in preparation) in the $\log(\text{H}\alpha/[\text{SII}])$ vs. $\log(\text{H}\alpha/[\text{NII}])$ diagnostic diagram by Cantó (1981). As shown in Fig. 3, the object falls in the lower left corner of the region occupied by bipolar PNe, far from the loci of HII regions and supernova remnants, and is characterized by extreme values of the $\text{H}\alpha/[\text{SII}]$ and $\text{H}\alpha/[\text{NII}]$ ratios. It has to be noted that the locus of bipolar PNe in this diagnostic diagram is, on the average, displaced toward higher $[\text{NII}]/\text{H}\alpha$ and $[\text{SII}]/\text{H}\alpha$ ratios as compared to the general sample of PNe.

3.4. Physico-chemical properties

The logarithmic extinction constant has been computed from the $\text{H}\alpha/\text{H}\beta$ ratio to be $c_\beta \sim 1.23$. By extrapolating the Galactic reddening maps by Neckel et al. (1980), this value gives an extinction distance of roughly 2 kpc, which is in agreement with the kinematical determination.

Electron density N_e and temperature T_e have been computed from the $[\text{SII}]671.7, 673.1$ doublet and the $[\text{NII}]658.4/[\text{NII}]575.5$ ratios, respectively, and are given in Table 2. The $[\text{OIII}]$ temperature, normally used in the calculation of the abundances for the high ionisation species, has been assumed to be equal to the $[\text{NII}]$ temperature. Given N_e and T_e , the ionic and total abundances of He, O, N, Ar and S relative to hydrogen have been computed from the line fluxes relative to $\text{H}\beta$, as described in Corradi et al. (1997). The computed abundances are given in Table 3. Considering the uncertainties in the observed fluxes and in the electronic temperature, we estimate that the errors on the total abundances are of the order of 20% for He, 50% for O, Ar, and S, and 70% for N. In spite of these large errors, very interesting results appear. While the O, Ar, and S abundances have, within errors, solar values, the nebula shows a substantial enrichment of helium ($\text{He}/\text{H} = 0.147 \pm 0.029$) and nitrogen ($\log N^+/O^+ \cong \log N/O = +0.47_{-0.38}^{+0.20}$). These numbers not only support our hypothesis that the nebula is the material ejected from an evolved star, but also indicate the occurrence of an extreme N enrichment, which is possibly (but see errors) the highest among PNe (cf. M 1–75, Guerrero et al. 1995, and the compilation in CS95). These He and N overabundances cannot be reproduced by the current models for AGB stars (cf. CS95).

Table 3. Chemical abundances (*icf* = ionisation correction factors).

| Ion/Elem. | Line | Abundance |
|---------------------------------------|--------------|--------------|
| He^+/H | 587.6 | 0.105 |
| He^{2+}/H | 468.6 | 0.042 |
| He/H | total | 0.147 |
| $\text{O}^0/\text{H} \times 10^4$ | 630.0 | 0.70 |
| | 636.4 | 0.45 |
| | mean | 0.53 |
| $\text{O}^+/\text{H} \times 10^4$ | 732.5 | 1.65 |
| $\text{O}^{2+}/\text{H} \times 10^4$ | 495.9 | 2.86 |
| | 500.7 | 2.97 |
| | mean | 2.92 |
| <i>icf</i> | | 1.25 |
| O/H $\times 10^4$ | total | 5.70 |
| $\text{N}^+/\text{H} \times 10^4$ | 575.5 | 4.94 |
| | 654.8 | 4.77 |
| | 658.3 | 4.94 |
| | mean | 4.87 |
| <i>icf</i> | | 3.46 |
| N/H $\times 10^4$ | total | 16.80 |
| $\text{Ar}^{2+}/\text{H} \times 10^6$ | 713.5 | 3.72 |
| <i>icf</i> | | 1.41 |
| Ar/H $\times 10^6$ | total | 5.23 |
| $\text{S}^+/\text{H} \times 10^6$ | 671.7 | 5.92 |
| | 673.1 | 5.91 |
| | mean | 5.92 |
| $\text{S}^{2+}/\text{H} \times 10^6$ | 631.2 | 17.68 |
| <i>icf</i> | | 1.16 |
| S/H $\times 10^6$ | total | 27.37 |

3.5. Temperature of the central star

We have estimated the colour temperature of the (unknown) exciting star by means of the Energy Balance method, following the recipes in Preite-Martinez & Pottasch (1983). The nebula has a high excitation class (5 or 6 according to the $[\text{OIII}]/\text{H}\beta$ and $\text{HeII}/\text{H}\beta$ ratios), and the contribution to the radiative cooling of unobserved UV and IR ions of C, O, S, and Ne can be significant. For this reason, only a lower limit of 130000 K can be derived.

4. Discussion

The properties of the nebula firmly support its classification as a PN. Morphologically, the degree of symmetry is not usually observed in galactic HII regions. Spectroscopically, the diagnostic diagram of Cantó (1981) locates it in the region of bipolar PNe; the spectrum is of high excitation corresponding to a very hot ionising source ($\log T > 5.1$); the He and N abundances are clearly enhanced as expected in evolved stars and observed especially in the class of bipolar PNe (CS95). The location of the nebula very close to the Galactic plane ($z \sim 70 \text{ pc}$) is consistent with the distribution of bipolar PNe, which are known to belong to a Galactic young disc population with a scale height of 130 pc (CS95). Following the nomenclature of Acker et al. (1992), the nebula should therefore be named as PN G321.6+02.2.

This object shows some extreme properties. With the adopted distance, it is possibly the largest PN (cf. CS95): the

symmetric hourglass nebula has a long axis of $\gtrsim 2.4$ pc, and the overall extent of the object is of $\gtrsim 4$ pc including the outer faint filaments (the lower limits are due to possible projection effects). Following the discussion in sect. 2.2 and assuming a polar expansion velocity $< 100 \text{ km s}^{-1}$, this gives a kinematical age of > 12000 yr. As for chemical abundances, it is clearly a Type I PN (Peimbert & Torres–Peimbert 1983), its He and N abundances being among the highest ever observed in PNe. Its large size, small gas densities, as well as the fact that the central star is very hot and faint, indicate that the nebula is in a very evolved evolutionary stage. The study of this kind of senile nebulae can be of great help in better understanding the PN phase and the post–AGB evolution of intermediate-mass stars.

References

- Acker, A., Ochsenbein, F., Stenholm, B., Tylenda, R., Marcout, J., Schohn, C.: 1992, Strasbourg–ESO catalogue of Galactic planetary nebulae, ESO
- Balick, B., Frank, A.: 1997, in Planetary Nebulae, IAU Symp. 180, in press
- Cantó, J.: 1981, in Investigating the Universe, Reidel, Dordrecht, p.95
- Corradi, R.L.M., Schwarz, H.E.: 1993, A&A 269, 462
- Corradi, R.L.M., Schwarz, H.E.: 1995, A&A 293, 871 (CS95)
- Corradi, R.L.M., Mampaso, A., Perinotto, M.: 1996, ESO Messenger, No.85, p. 37
- Corradi, R.L.M., Perinotto, M., Schwarz, H.E., Claeskens, J.-F.: 1997, A&A, in press
- Guerrero, M.A., Stanghellini, L., Machado, A.: 1995, ApJ 444, L49
- Livio, M.: 1997, in Planetary Nebulae, IAU Symp. 180, in press
- Machado, A., Guerrero, M.A., Stanghellini, L., Serra-Ricart, M.: 1996, ‘The IAC Morphological Survey of Northern Galactic PNe’, IAC Publ.
- Marsalkowa, P.: 1974, Ap&SS 27, 3
- Neckel, Th., Klare, G., Sarcander, M.: 1980, A&AS 42, 251
- Neckel, Th., Vehrenberg, H.: 1990, Atlas of Galactic Nebulae, Verlag
- Peimbert, M., Torres–Peimbert, S.: 1983, in Planetary Nebulae, IAU Symp. 103, Flower ed., p.233
- Preite–Martinez, A., Pottasch, S.R.: 1983, A&A 126, 31
- Solf, J., Ulrich, H.: 1985, A&A 148, 274